

MODE I INTERLAMINAR FRACTURE TOUGHNESS OF CARBON NANOTUBE WEB-MODIFIED POLYMER COMPOSITES

Ravi Chitwan¹, Andres Nistal¹, Brian G. Falzon^{1*} and Stephen C. Hawkins^{1,2}

¹ School of Mechanical and Aerospace Engineering, Queen's University Belfast, UK, BT9 5AH,

Email: rchitwan01@qub.ac.uk, Web Page: <http://www.qub.ac.uk>

Email: a.nistal@qub.ac.uk, Web Page: <http://www.qub.ac.uk>

Email: b.falzon@qub.ac.uk, Web Page: <http://www.qub.ac.uk>

Email: Stephen.Hawkins@qub.ac.uk, Web Page: <http://www.qub.ac.uk>

²Department of Materials Engineering, Monash University, Clayton, Victoria, Australia, 3800

Email: Stephen.Hawkins@monash.edu, Web Page: <http://eng.monash.edu.au>

Keywords: Carbon nanotube web, interlaminar fracture toughness, Toughened epoxy resin, Multifunctional hierarchical composites.

ABSTRACT

Carbon nanotube 'webs' (CNTWs) are used as interlayers between marine grade (HMC/SE84LV) and aerospace grade (IM7/977-2) carbon fibre-reinforced polymer (CFRP) composite laminates to explore their influence on mode I interlaminar fracture toughness (ILFT). Inserting CNTW in SE84LV laminates improves the mode I ILFT by 4% whereas inserting CNTW in 977-2 laminates reduces the mode I ILFT by 85%. Fractography and interfacial analysis show that SE84LV resin penetrated and adequately wetted the CNTW whereas 977-2 resin failed to penetrate and wet the CNTW which resulted in large void formation and created a weak interlaminar region. To counter the poor penetration of 977-2 resin, CNTW was impregnated with neat 977-2 resin prior to its insertion in the prepreg layup. Inserting preimpregnated CNTW resulted in a 68% reduction in mode I ILFT. It is proposed that the reduction in mode I ILFT of IM7/977-2 system interleaved with CNTW was due to the restricted resin mobility in the CNTW region and the poor interaction between CNTW and 977-2 resin. The 977-2 remains at minimum viscosity for a shorter time than SE84LV. Remaining at low viscosity for a longer period allows the resin to flow in the CNTW region. The weak interaction between CNTW and the 977-2 resin is discussed in terms of the polarity of the constituent polymer molecules. 977-2 is more polar than SE84LV thus has a very low affinity to interact with CNTW.

1 INTRODUCTION

Carbon fibre-reinforced polymer (CFRP) composites are widely used in the primary structure of the current generation of civil aircraft, comprising for example - 50 wt. % and 53 wt. % of the airframes of the Boeing 787 Dreamliner [1] and the Airbus A350XWB [2], respectively. Composites are preferred over traditional aluminium alloy due to their superior specific strength and stiffness, high corrosion and fatigue resistance [3]. However, CFRP composites have poor through-thickness fracture toughness which makes them susceptible to delamination damage.

Various forms of carbon nanotube (CNT) assemblies (e.g. CNT forests [4], dispersed CNTs [5] and directly grown CNTs on fibres [6]) are being studied to deliver improved electrical and thermal management, sensing as well as improved interlaminar fracture toughness (ILFT) to composite materials. The focus on CNTs is mainly due to their small size, low density, exceptional mechanical, electrical and thermal properties, high aspect ratio and large specific surface area. CNTs have a distinct electrical response to applied load [7]. Thus they are proposed as lightweight heating elements for anti-/de-icing capability [8] and sensors for in-situ structural health monitoring (SHM) in composite airframes. CNTs have also been used as fillers in resin to improve its electrical [9], mechanical [10] and thermal properties [11]. However, utilisation of their properties to their full potential is limited by their susceptibility to agglomerate within the polymer [12] and difficulty to grow the CNTs directly on reinforcing fibres without damaging them [13].

A CNT 'web' or continuous ribbon of horizontally aligned nanotubes drawn from specially grown vertically-aligned-CNT forests is a uniquely useful and adaptable form of CNTs. The CNT web (CNTW) has great potential for improving the functionality of CFRP composites. However delamination is an 'Achilles's heel' of laminates so any addition of another material must at least maintain the CFRP performance and preferably enhance it, in addition to creating the additional functionality desired. This study investigates the effect on 'Mode I' interlaminar fracture toughness (ILFT) of CFRP composites when using CNTW between the laminates.

2 EXPERIMENTAL METHODOLOGY

2.1 Materials

Composite specimens were prepared using unidirectional high modulus carbon fibre, HMC/SE84LV prepreg, from Gurit and IM7/977-2 prepreg, from Solvay. SE84LV is a patented marine grade thermoplastic-toughened epoxy resin system, having two bi-functional epoxy monomers [14], [15]. CYCOM 977-2 is a proprietary aerospace grade polyethersulfone-based poly-aromatic thermoplastic toughened epoxy resin system. It has two bi-functional and one tri-functional epoxy monomers along with 4,4-diaminodiphenyl sulfone (DDS) hardener [16], [17].

CNTWs were prepared by drawing from a high-specification CNT forest [18] and winding continuously onto a support frame to a thickness of 10 layers. The MWCNTs have a high aspect ratio of over 30,000. CNTs have 7 ± 3 walls with an approximate diameter of 10 nm and approximate length of 300 μm . A single layer of CNTW has an aerial density of approximately 0.02 g/m². The CNT forests are grown, on silicon substrates, with a 50 nm thermal oxide and 2.5 nm e-beam deposited catalyst, by CVD using acetylene and hydrogen (each 2.5%) in helium at 1 slm total within a 44 mm inner diameter quartz reactor at 690 °C for 12 minutes [19].

2.2 Drawing of CNTWs

Support frames (90 mm x 90 mm with a 70 mm square opening), mounted on plastic blocks were rotated using an electric motor. MWCNTs were drawn perpendicular to the forest and wound on the frames, (Fig. 1a). Ten rotations of the blocks gave 10 layer of CNTWs.

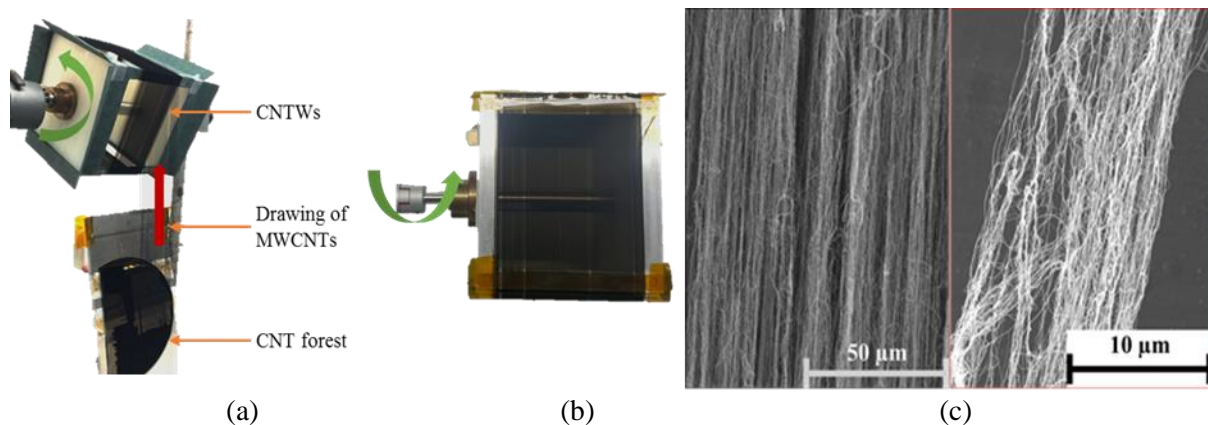


Figure 1: (a) CNT winding, (b) CNTWs (c) scanning electron micrograph of CNTW (top view).

2.3 Embedding of CNTWs into the prepreg plies and prepreg layup procedure

The layered CNTWs (70 mm x 70 mm) were directly transferred onto the midplane of prepreg laminates, (Fig. 2a). The CNT draw direction was at 90° to the UD carbon fibre. Every layup contained a combination of control specimens (e.g. CNT free, pristine CNTW, resin impregnated CNTW, neat resin film insertion, etc.) In the case of IM7/977-2, some CNTWs were impregnated with neat 977-2 resin prior to embedding (Fig. 2b) to ensure effective penetration and wetting. Thus release-paper containing 20 μm thick 977-2 resin film was placed underneath the CNTWs and heated to 100 °C for

30 seconds which resulted in the resin fully penetrating the CNTWs. Neat resin film was inserted separately in the composite layup forming a secondary control specimen for this case (Fig. 2a).

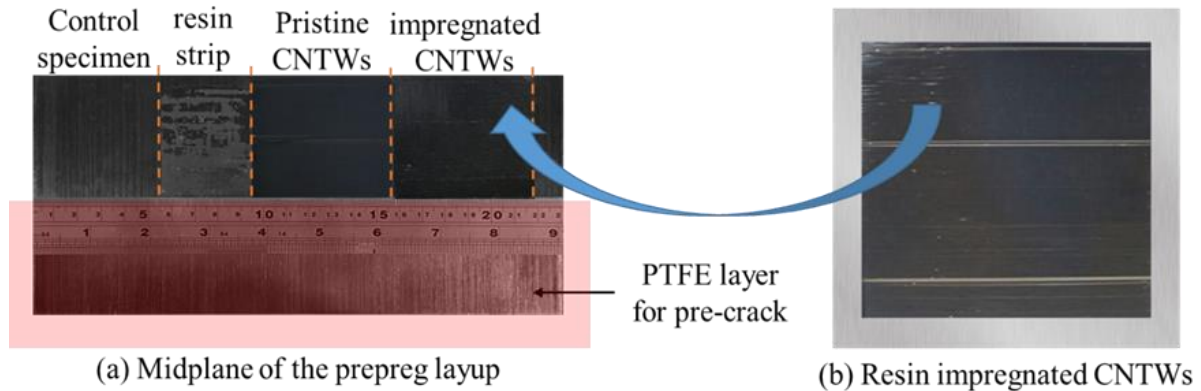


Figure 2: (a) Embedding of CNTWs (b) resin impregnated 10 layer CNTW.

2.4 Compression moulding and DCB specimen preparation

Once the prepreg layup was completed, the composite laminates were cured according to manufacturers' recommendations [16], [20]. The HMC/SE84LV layup was heated from 30 °C to 120 °C with 1 hr dwell time. The IM7/977-2 layup was heated from 30 °C to 177 °C with 3 hrs dwell time. The ramp rate for both samples was set to 2 °C/min. After completion, the composite panels were demoulded and 20 mm wide double cantilever beam (DCB) specimens were cut. The DCB specimens for mode I tests were prepared in accordance with ASTM D5528 [21]. Piano hinges were attached to the pre-cracked ends of the specimen to grip it to the mechanical testing machine.

2.5 Characterisation

DCB specimens were tested (Instron 5564, 5 kN load cell) at 2 mm/min. Microscope cameras were placed on either sides of the specimen to track the crack tip against calibration marks and ensure the stability of the crack-front. Applied load (P) and opening displacement (δ) were measured to calculate the Mode I ILFT, G_{IC} , using the modified compliance calibration (MCC) method [21]. The equations used for this purpose are stated below [21],

$$G_{IC} = \frac{3P^2 C^{2/3}}{2A_1 b h} \times F, \quad (1)$$

where C is the compliance of the DCB specimen, given as,

$$C = \delta/P, \quad (2)$$

A_1 is the slope of the plot of a/b versus $C^{1/3}$, where a , is the delamination (crack) length, b , is the width of the specimen, h , is the thickness of the DCB specimen and F , is the displacement correction factor given by,

$$F = 1 - \frac{3}{10} \left(\frac{\delta}{a} \right)^2 \left(\frac{\delta t}{a^2} \right), \quad (3)$$

where t , is the distance from loading block pin to centre line of the top specimen arm.

Scanning electron microscopy, (SEM, FlexSEM 1000, Hitachi) was used for fractography and interfacial thickness and void content analysis. SEM was used in secondary electron mode. Up to 10 kV of current was supplied to the sample at a working distance of 5 mm. The spot intensity was set to 70 for low magnification and 30 for high magnification microscopy. The fracture surface was sputtered with 5 nm thick layer of gold.

Differential scanning calorimetry, (DSC, DSC-6, PerkinElmer) was used for thermal analysis. In dynamic scanning mode, the sample was heated from 30 °C to 350 °C at a rate of 10 °C/min whereas, in isothermal scanning mode, the sample was heated and dwelled in accordance with the supplier's recommended curing profile to mimic the thermal behaviour of resins during curing process.

3 RESULTS AND DISCUSSION

3.1 Mode I interlaminar fracture toughness

The pristine CNTW-modified HMC/SE84LV composite showed a 4% increase in mode I performance when compared to the control sample, with 95% confidence level, (Fig. 4a, Table 1). However, the pristine CNTW-modified IM7/977-2 composite showed a degradation of 85% in mode I strength when compared to its control sample, (Fig. 4b, Table 1). This poor result was attributable to the failure of the resin to fully penetrate and wet the CNTW interlayer. The neat 977-2 resin film-insert showed 10% reduction in mode I performance whereas the 977-2 resin film impregnated CNTW showed a 64% degradation in mode I ILFT. Results are shown in Table 1.

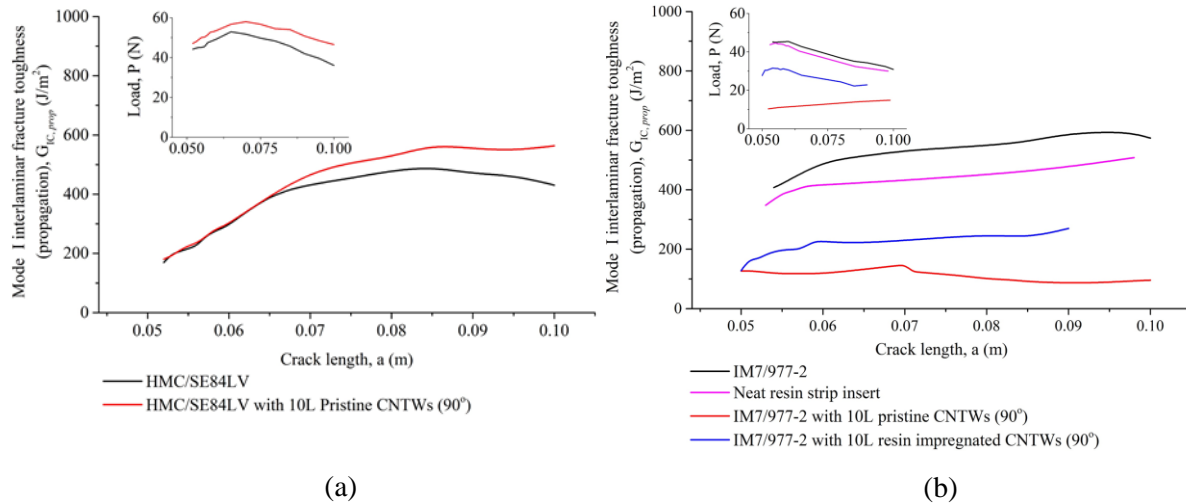


Figure 4: Mode I ILFT along with respective load versus crack length plot of 10 layer CNTW-modified (a) HMC/SE84LV and (b) IM7/977-2 composite laminates.

Material	Specimen	Avg. mode I interlaminar fracture toughness, $G_{IC,prop}$ (J/m ²)	Number of samples	Change, (%)
HMC/SE84LV	Control	348 ± 22	8	-/-
	Pristine CNTWs	362 ± 29	6	+4
IM7/977-2	Control	550 ± 45	18	-/-
	Pristine CNTWs	82 ± 15	6	-85
	20 μm resin strip insert	495 ± 26	12	-10
	Resin impregnated CNTWs	200 ± 18	6	-64

Table 1: Average mode I interlaminar fracture toughness of 10 layer CNTW-modified laminates.

3.2 Fractography

Fracture morphology of specimens was studied in order to understand the presence or absence of toughening mechanisms corresponding to change in mode I ILFT. Figure 5a-5c and 5d-5f show the fracture surfaces of a HMC/SE84LV control and CNTW-modified specimens, respectively.

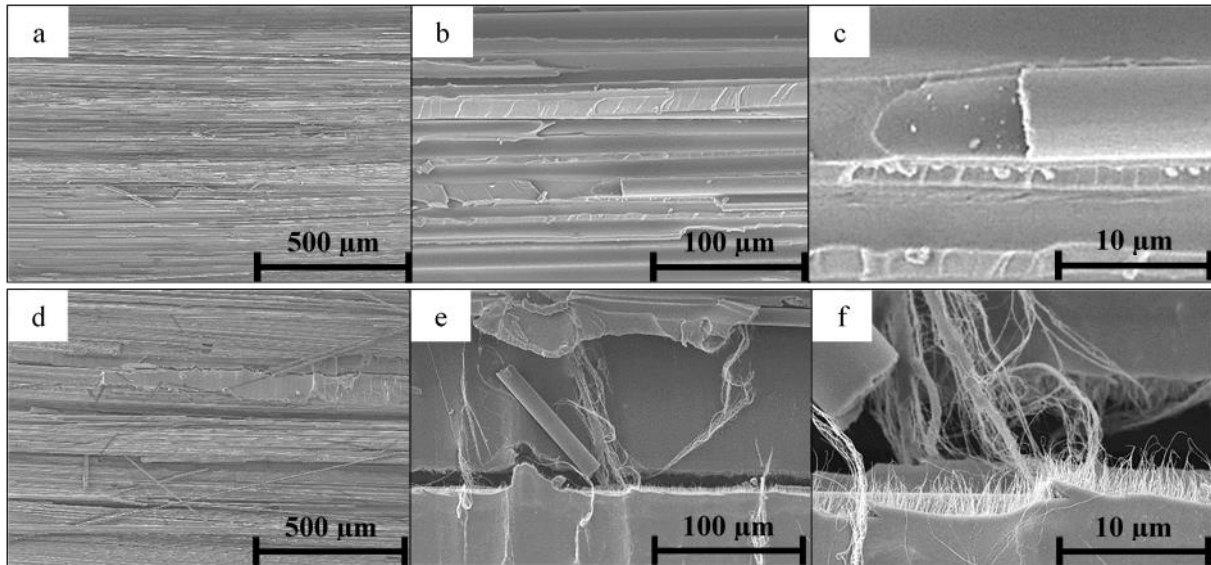


Figure 5: Fracture surface of (a) HMC/SE84LV control and (b) 10-layer pristine CNTW-modified specimens.

Although mode I delamination is a matrix dominant failure, some fragmented carbon fibres were observed on both fracture surfaces, (Fig. 5a and 5d), confirming the occurrence of fibre bridging, which is a toughening mechanisms common in UD CFRP laminates [22]. Crack pinning ‘tails’ are evident, which were formed during crack propagation through the thermoplastic phase [23] (Fig. 5b and 5e). Cusps and ribbons were also observed which signify ductile failure regions on the fracture surface, (Fig. 5a and 5b)[22]. In the case of CNTW-modified HMC/SE84LV specimen (Fig 5d-5f), the CNT-matrix interface was observed one fibre-layer below the fracture surface. It is a mixed mode fracture where crack jumps from one interface to the other were observed [23]. Small patches of CNTW-matrix interface were visible on the fracture surface, (Fig 5e) which indicate crack deflection from tougher CNTW-modified interlaminar region to a weaker ‘control specimen-like’ interlaminar region. It was observed that thermoplastic fibrils [23] were reinforced with CNTW, (Fig. 5e and 5f). CNT bridging and CNT pullouts are evident from the micrographs which confirm effective load transfer from the matrix to nanotubes. It is evidence of adequate wetting of the CNTW assembly by the resin present on the surface of adjoining prepreg plies and strong CNT-SE84LV interaction. These factors contribute to the observed 4% increase in mode I ILFT.

The IM7/977-2 control specimen, (Fig 6a-6c) shows the same suite of toughening features as the SE84LV. Pristine CNTW-modified IM7/977-2 laminate showed no fibre bridging, (Fig. 6d-6f) but rather a smooth fracture surface representing weak cohesive fracture [23], where the crack propagated easily throughout the CNTW-matrix interface (Fig. 6d). Large voids were also observed on the fracture surface, (Fig. 6f), [24] and clearly the 977-2 resin failed to penetrate the CNTWs resulting in an 85% reduction in mode I ILFT.

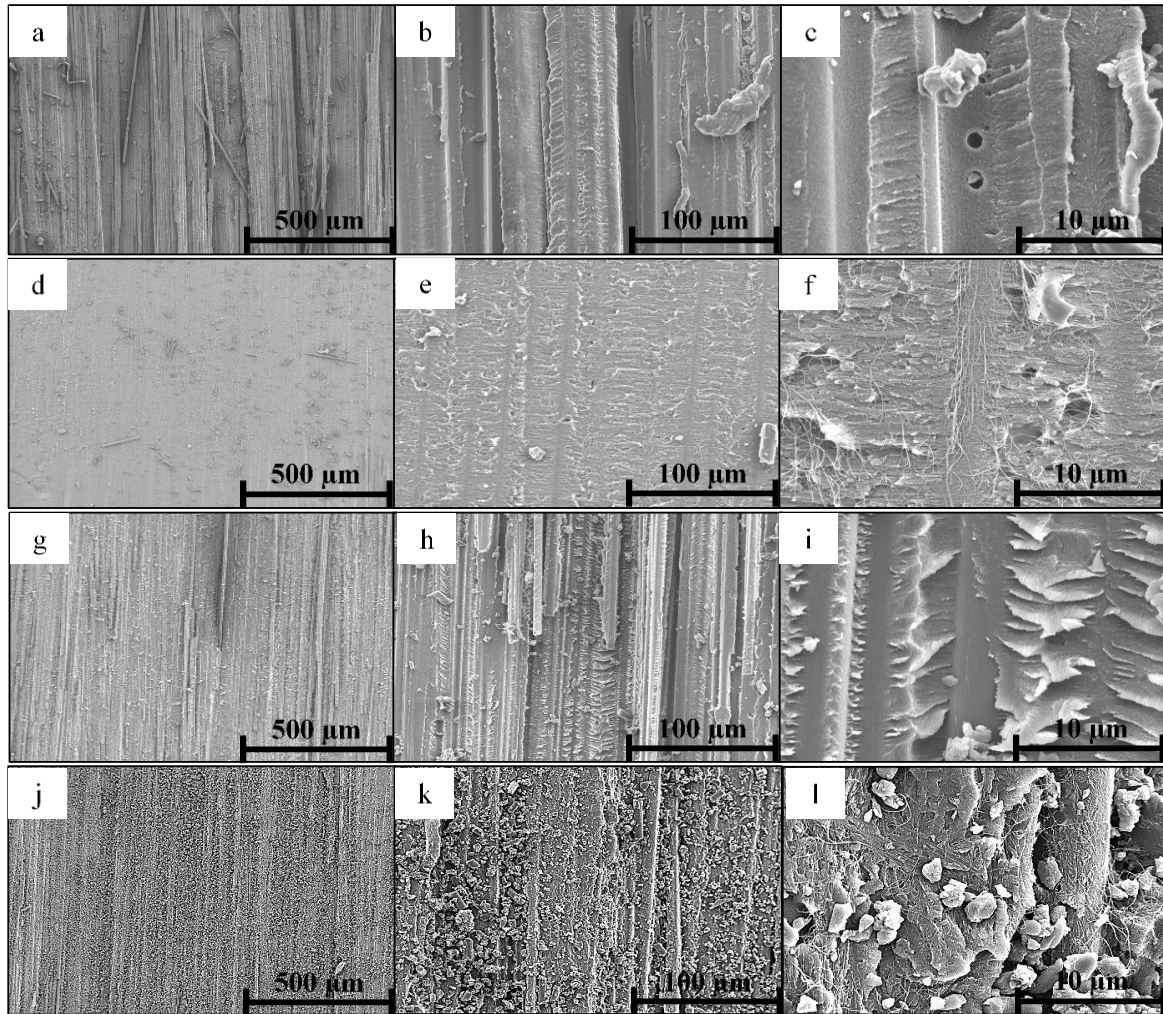


Figure 6: Fracture surface of (a) IM7/977-2 control, (b) pristine CNTW-modified IM7/977-2, (c) resin strip-insert and (d) resin impregnated CNTW-modified IM7/977-2 specimens.

In order to improve the wetting of CNTWs, they were impregnated with 977-2 resin film prior to insertion. A secondary control specimen containing the neat resin film was also created. Brittle fractured resin debris was observed on the fracture surface of the resin-modified specimen, (Fig. 6g-6i). It is likely that excess resin did not bleed out of the prepreg system completely. The rest of the fracture features were similar to the control specimen. These specimens exhibited a 10% reduction in mode I interlaminar fracture toughness.

In the case of resin impregnated CNTW-modified IM7/977-2 specimens, the fracture morphology was mostly a combination of that of pristine CNTW-modified and resin-modified specimens, absence of fibre bridging, CNT pullout, CNT bridging and the presence of brittle fracture resin debris, (Fig. 6j-6l). A distinctive feature was observed at higher magnification, several CNT imprints were formed on the surface of cured 977-2 matrix, (Fig. 7). It is conceived that excess molten resin penetrates and wets the CNTW assembly but does not interact with it. It is an indication of poor interaction between CNTW and 977-2 resin. It can be inferred from observations that this poor interaction reverses the role of CNTWs from being a reinforcement into defect.

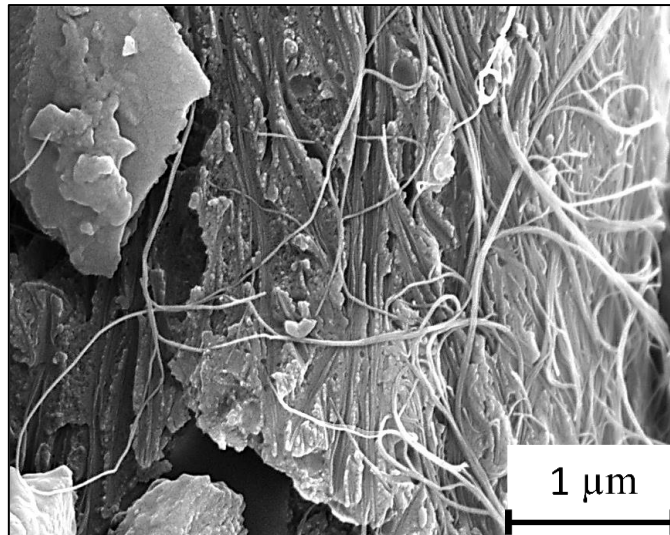


Figure 7: Fracture surface of resin impregnated CNTW-modified IM7/977-2 specimen.

3.3 Analysis of CNTW-matrix interface

This section quantifies the change in interlaminar thickness and the increase in void content upon inclusion of carbon nanotube webs (Fig. 8, Table 2). As shown, when 10 layers of pristine CNTWs were inserted in HMC/SE84LV laminate, the interlaminar thickness the specimen increased by approximately 2 μm , (Table 2, Fig. 8a and 8b). The void content increased by 0.1% but the average void size remained the same, (Table 2). It affirms the observation that the CNTWs were adequately wetted by SE84LV resin during cure.

On the other hand, the IM7/977-2 control specimen had no distinct interlaminar region, (Fig. 8c). A homogenous carbon fibre-resin interface was observed. But when pristine CNTWs were inserted in IM7/977-2 specimen, a $1 \pm 0.5 \mu\text{m}$ thick, porous CNTW-matrix interface was formed, (Table 2). It is noted that the 977-2 resin failed to penetrate into the CNTW assembly, (Fig. 8d). Furthermore, when 20 μm thick resin film was inserted in between the plies, the interlaminar thickness increased from 0 to 10 μm , (Table 2). It is confirmed from the interfacial analysis that excess resin did not bleed out of the IM7/977-2 system during the curing process, (Fig. 8e). The 'resin-rich' interlaminar region resulted in 10% reduction of mode I strength. The void content and average void size in the resin-modified specimen was similar to that of the control specimen. Furthermore, the resin impregnated CNTW-matrix interface was seen to have similar thickness as the resin-modified specimen but the void content in resin impregnated CNTW specimen increased to 2.2% with an average void/defect size of $3.6 \pm 2.7 \mu\text{m}$, (Fig. 8f, Table 2). This 175% increase in average defect size is correlated with the fractography observations that suggests, poor interaction between CNTW and 977-2 matrix is the reason for the 64% decrease in mode I strength.

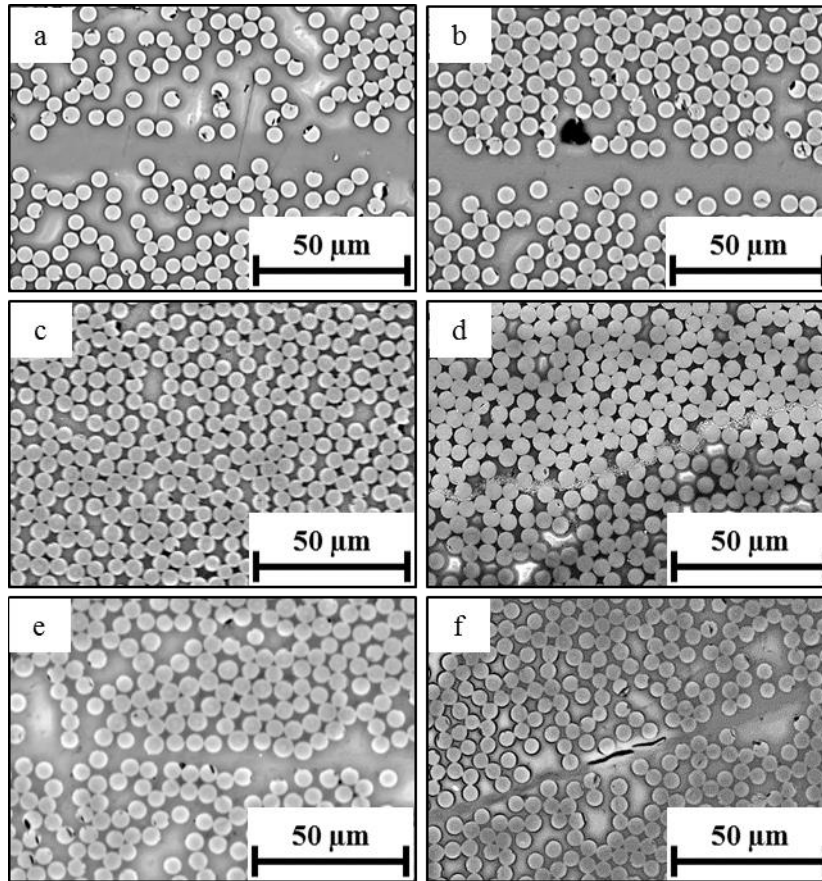


Figure 8: Cross-section of (a) HMC/SE84LV control, (b) pristine CNTW-modified HMC/SE84LV, (c) IM7/977-2 control, (d) pristine CNTW-modified IM7/977-2, (e) resin strip-insert and (f) resin impregnated CNTW-modified IM7/977-2 specimens.

Material	Specimen	Interlaminar thickness \pm s.d. (μm)	Void (%)	Average void size \pm s.d. (μm)
HMC/SE84LV	Control	8 ± 2	0.7	2.5 ± 0.9
	Pristine CNTWs	10 ± 4	0.8	2.5 ± 1.9
IM7/977-2	Control	*	0.9	1.5 ± 0.1
	Pristine CNTWs	1 ± 0.5	†	†
	20 μm resin strip insert	10 ± 4	0.8	1.5 ± 0.3
	Resin impregnated CNTWs	10 ± 6	2.2	3.6 ± 2.7

* No distinct interlaminar region was observed.

† Void content and void size could not be calculated due to very porous CNTW-matrix interface.

Table 2: Interlaminar thickness and void content in specimens.

3.4 Viscosity change and thermal analysis of epoxy resins

From the experimental data provided in the literature it is observed that SE84LV reaches a minimum viscosity of 2.9 Pa-s at 99 °C whereas, the 977-2 reaches a minimum viscosity of 1.1 Pa-s at 157 °C when heated at 10 °C/min. In comparison to SE84LV, the viscosity of 977-2 resin at 99 °C is 10 Pa-s. The viscosity curve of both resins have approximately similar slope until the minimum viscosity is achieved. However, the viscosity of 977-2 increases rapidly beyond the point of minimum viscosity during gelation [25].

The thermal behaviour of resins was studied using dynamic and isothermal DSC plots, (Fig. 9a and 9b). The total heat of reaction, ΔH_{max} , was measured from the dynamic scans; 977-2 resin released 302

J/g of heat which is 3.5 times greater than total heat released by SE84LV resin during dynamic DSC. A high amount of heat released suggests a high exotherm reaction experienced by 977-2 resin during crosslinking. As a result, it accelerates the epoxy-ring opening and polymer network formation, [26]. It is calculated from the isothermal test that 977-2 resin takes nearly 60 minutes to reach 95% cure whereas SE84LV takes 50 minutes to reach 95% cure, at respective curing temperatures. CYCOM 977-2 is a high-temperature-cure resin system, containing a mixture of a phenol formaldehyde-based bi-functional epoxy, a bisphenol F-based bi-functional epoxy and an aniline-based tri-functional epoxy with 4,4-diaminodiphenyl sulfone (DDS) curing agent. On the other hand, SE84LV is a relatively less complex system containing one bisphenol A-based epoxy and one bisphenol F-based epoxy monomer along with proprietary thermoplastic toughener and hardener.

Comparatively, there are more monomers in the 977-2 resin system, which may take longer time to crosslink. It is suggested that the synergy among the epoxy monomers, thermoplastic and curing agent is such that, un-functionalised non-polar carbon nanotubes have very low affinity to chemically interact with the more polar 977-2 resin during the curing process, [27]. Since the SE84LV resin is less polar, it has an affinity to interact with the pristine carbon nanotubes. This is a proposed reason for the poor interaction between 977-2 resin and CNTWs derived from observing the thermal characteristics of the resins and their chemical formulation analysis.

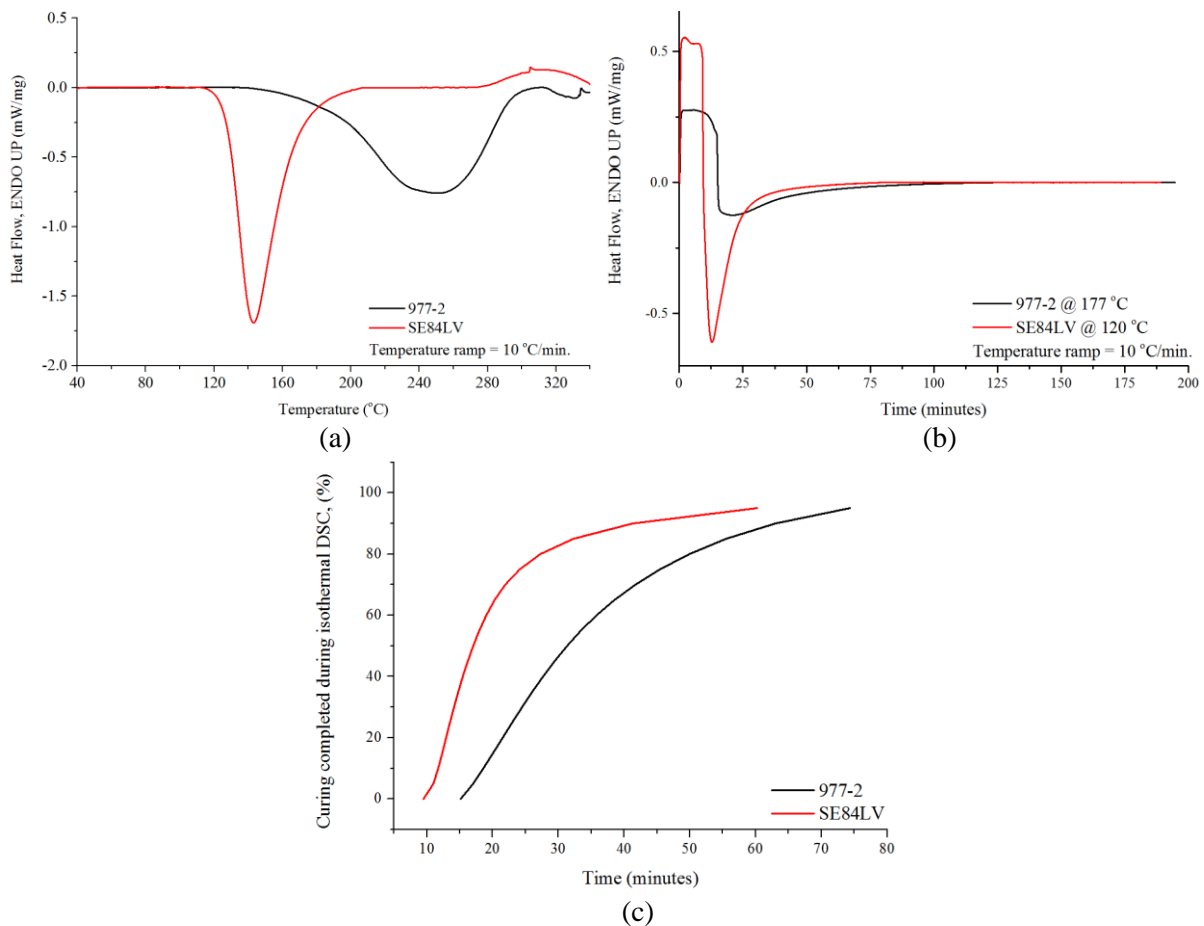


Figure 9: Thermal response of toughened epoxy resin systems SE84LV and 977-2 in (a) Dynamic and (b) Isothermal scanning mode of DSC and (c) curing versus time relationship.

4 CONCLUSION

The CNTWs behave differently in comparatively lower performance (SE84LV) and higher performance (977-2) toughened epoxy resin systems. The mode I ILFT of the CFRP laminates was directly influenced by the quality of the CNTW-matrix interface. Poor penetration of 977-2 resin in

CNTWs interlayer resulted in large void formation which weakened the CNTW-matrix interface and degraded the mode I strength of the laminate. This poor penetration of resin and wettability of the CNTWs may be explained in terms of the thermal and chemical characteristics of the epoxy resins. The total heat released by 977-2 resin during curing was 3.5 times higher than that of SE84LV resin. It is suggested that the 977-2 system experiences higher exotherm during crosslinking which accelerates the rate of polymer network formation while the presence of highly polar 977-2 polymer molecules are likely to adversely affect its chemical interaction with the nonpolar CNTW. It is therefore recommended that an in-depth study of the physical and chemical interactions between CNTs and complex thermoplastic toughened epoxy resin systems is undertaken prior to deploying CNT-based assemblies as multifunctional fillers in aerospace composites.

ACKNOWLEDGEMENT

This work was supported by the UK Engineering and Physical Sciences Research Council (EPSRC) grant EP/N007190/1. The corresponding author would like to acknowledge the financial support of Bombardier and the Royal Academy of Engineering.

REFERENCES

- [1] J. Fraga, "Boeing 787 from the Ground Up," *AERO Mag.*, pp. 17–23, 2006.
- [2] R. Thevenin, "Composites in Airbus," *Glob. Invest. Forum*, pp. 1–26, 2008.
- [3] J. Njuguna, K. Pielichowski, and J. R. Alcock, "Epoxy-based fibre reinforced nanocomposites," *Adv. Eng. Mater.*, vol. 9, no. 10, pp. 835–847, 2007.
- [4] D. J. Kovach, K. H. Griess, N. Yamamoto, R. G. DeVilloria, H. G. Cebeci, and B. L. Wardle, "Thermal and electrical transport in hybrid woven composites reinforced with aligned carbon nanotubes," Seattle, Washington, 2013.
- [5] B. F. Jogi, "Dispersion and Performance Properties of Carbon Nanotubes (CNTs) Based Polymer Composites: A Review," *J. Encapsulation Adsorpt. Sci.*, vol. 2, no. 4, pp. 69–78, 2012.
- [6] S. P. Sharma and S. C. Lakkad, "Effect of CNTs growth on carbon fibers on the tensile strength of CNTs grown carbon fiber-reinforced polymer matrix composites," *Compos. Part A Appl. Sci. Manuf.*, vol. 42, no. 1, pp. 8–15, 2011.
- [7] I. Kang, M. J. Schulz, J. H. Kim, V. Shanov, and D. Shi, "A carbon nanotube strain sensor for structural health monitoring," *Smart Mater. Struct.*, vol. 15, no. 3, pp. 737–748, 2006.
- [8] O. Gohardani, M. C. Elola, and C. Elizetxea, "Potential and prospective implementation of carbon nanotubes on next generation aircraft and space vehicles: A review of current and expected applications in aerospace sciences," *Progress in Aerospace Sciences*, vol. 70, pp. 42–68, 2014.
- [9] J. Sandler, M. S. . Shaffer, T. Prasse, W. Bauhofer, K. Schulte, and A. . Windle, "Development of a dispersion process for carbon nanotubes in an epoxy matrix and the resulting electrical properties," 1999.
- [10] Z. K. Chen, J. P. Yang, Q. Q. Ni, S. Y. Fu, and Y. G. Huang, "Reinforcement of epoxy resins with multi-walled carbon nanotubes for enhancing cryogenic mechanical properties," *Polymer (Guildf.)*, vol. 50, no. 19, pp. 4753–4759, 2009.
- [11] F. H. Gojny, M. H. G. Wichmann, B. Fiedler, I. A. Kinloch, W. Bauhofer, A. H. Windle, and K. Schulte, "Evaluation and identification of electrical and thermal conduction mechanisms in carbon nanotube/epoxy composites," *Polymer (Guildf.)*, vol. 47, no. 6, pp. 2036–2045, 2006.
- [12] D.-L. Shi, X.-Q. Feng, Y. Y. Huang, K.-C. Hwang, and H. Gao, "The Effect of Nanotube Waviness and Agglomeration on the Elastic Property of Carbon Nanotube-Reinforced Composites," *J. Eng. Mater. Technol.*, vol. 126, no. July, p. 250, 2004.
- [13] V. P. Veedu, A. Cao, X. Li, K. Ma, C. Soldano, S. Kar, P. M. Ajayan, and M. N. Ghasemi-Nejhad, "Multifunctional composites using reinforced laminae with carbon-nanotube forests.," *Nat. Mater.*, vol. 5, no. 6, pp. 457–462, 2006.
- [14] Gurit (UK) Ltd., "SE84LV Material Safety Data Sheet," Newport, UK, 2008.
- [15] P. J. Spencer, G. J. Edwards, and K. V. Redrup, "Carbon Fibre-Containing Prepregs," US 2016/0083543 A1, 2016.
- [16] E. Atures and P. Ations, "Cycom 977-2 Epoxy Resin System -Technical Data Sheet," *Cytec* -

- Engineered Materials*, 2012. [Online]. Available: <http://www.cemselectorguide.com/>
[Accessed: 10-Nov-2014].
- [17] L. H. Strait, M. L. Karasek, and M. F. Amateau, "Effects of Stacking Sequence on the Impact Resistance of Carbon Fiber Reinforced Thermoplastic Toughened Epoxy Laminates," *J. Compos. Mater.*, vol. 26, no. 12, pp. 1725–1740, 1992.
- [18] B. G. Falzon, S. C. Hawkins, C. P. Huynh, R. Radjef, and C. Brown, "An investigation of Mode I and Mode II fracture toughness enhancement using aligned carbon nanotubes forests at the crack interface," *Compos. Struct.*, vol. 106, pp. 65–73, Dec. 2013.
- [19] C. P. Huynh and S. C. Hawkins, "Understanding the synthesis of directly spinnable carbon nanotube forests," *Carbon N. Y.*, vol. 48, no. 4, pp. 1105–1115, 2010.
- [20] Gurit (UK) Ltd., "SE 84LV - Low Temperature Cure Epoxy Prepreg," *General Datasheet*, 2016. [Online]. Available: www.gurit.com.
- [21] ASTM Standard D5528 - 01, "Standard Test Method for Mode I Interlaminar Fracture Toughness of Unidirectional Fibre-Reinforced Polymer Matrix Composites," West Conshohocken, PA, USA, 2014.
- [22] E. Greenhalgh, M. Hiley, and C. Meeks, "Failure Analysis and Fractography of Polymer Composites," *Analysis*, no. March, p. 595, 2010.
- [23] A. Zotti, S. Zuppolini, M. Zarrelli, and A. Borriello, "Fracture Toughening Mechanisms in Epoxy Adhesives," in *Adhesives - Applications and Properties*, A. Rudawska, Ed. InTech, 2016, pp. 237–269.
- [24] Y. Li, Q. Li, and H. Ma, "The voids formation mechanisms and their effects on the mechanical properties of flax fiber reinforced epoxy composites," *Compos. Part A Appl. Sci. Manuf.*, vol. 72, pp. 40–48, 2015.
- [25] M. L. Costa, E. C. Botelho, J. M. F. De Paiva, and M. C. Rezende, "Characterization of cure of carbon/epoxy prepreg used in aerospace field," *Mater. Res.*, vol. 8, no. 3, pp. 317–322, 2005.
- [26] K. Haman, P. Badrinarayanan, and M. R. Kessler, "Cure characterization of the ring-opening metathesis polymerization of linseed oil-based thermosetting resins," *Polym. Int.*, vol. 58, no. 7, pp. 738–744, 2009.
- [27] a Carre, "Polar interactions at liquid/polymer interfaces," *J. Adhes. Sci. Technol.*, vol. 21, no. 10, pp. 961–981, 2007.